Direct radiative effects of dust aerosols emitted from the Tibetan Plateau on the East Asian summer monsoon – a regional climate model simulation

Hui Sun[1], Xiaodong Liu[1,2], and Zaitao Pan[3,4]

5   [1]SKLLQG, Institute of Earth Environment, Chinese Academy of Sciences, Xi'an, 710061, China
[2]CAS Center for Excellence in Tibetan Plateau Earth Sciences, Beijing, 100101, China
[3]Department of Earth and Atmospheric Sciences, Saint Louis University, St.Louis, Missouri, MO 63108, USA
[4]Key Laboratory of Meteorological Disaster, Ministry of Education, Nanjing University of Information Science and Technology, Nanjing, Jiangsu, China

10   *Correspondence to*: H. Sun (sunhui@ieecas.cn)

Abstract. While dust aerosols emitted from major Asian sources such as Taklimakan and Gobi Deserts have been shown to have strong effect on Asian monsoon and climate, the role of dust emitted from Tibetan Plateau (TP) itself, where aerosols can directly interact with the TP "heat pump" because of their physical proximity both in location and elevation, has not been examined. This study uses the dust coupled RegCM4.1 regional climate model to simulate the spatiotemporal distribution of dust aerosols originating in the TP and their radiative effects on the East Asian summer monsoon (EASM) during both heavy and light dust years. Two 20-year simulations with and without the dust emission from TP showed that direct radiative cooling in the mid-troposphere induced by the TP locally produced dust aerosols resulted in an overall anticyclonic circulation anomaly in the low-troposphere centered over the TP region. The northeasterly anomaly in the EASM region reduces its strength considerably. The simulations found a significant negative correlation between the TP column dust load produced by local emissions and the corresponding anomaly in the EASM index ($r=-0.41$). The locally generated TP dust can cause surface cooling far downstream in eastern Mongolia and northeastern China through stationary Rossby wave propagation. Although dust from within TP (mainly Qaidam Basin) is a relatively small portion of total Asian aerosols, its impacts on Asian monsoon and climate seems disproportionately large, likely owing to its higher elevation within TP itself.

25   ## 1 Introduction

Dust is one of the most important components of atmospheric aerosols. The main source of atmospheric dust is wind erosion in arid and semi-arid regions; it is estimated that the global atmospheric dust emission may be as high as 200–5000 Mt yr^{-1} (Goudie, 1983). Because of the large amount in the atmosphere, dust effects on the environment and the climate system have attracted much attention. The inhalation of dust aerosols can harm both human and animal health; it can also affect visibility and thus potentially increase the number of traffic accidents (Park and Kim, 2005). Dust aerosols

also are important drivers of the global climate because of their direct radiative effects on the Earth–atmosphere radiation balance and temperature (Tegen and Lacis, 1996; Miller et al., 2004). They can alter the atmospheric hydrological cycle by acting as cloud condensation nuclei and thus can modulate both the regional and global precipitation (Rosenfeld, 2001). Satellite observations have shown that dust originating from the Taklimakan Desert can travel around the globe within two weeks and alter the interaction between the atmospheric CO_2 and the global climate by providing nutrients to and interacting with the marine ecosystem (Uno et al., 2009).

East Asia is an important source region for dust (Zhang et al., 1996) and is home to more than half of the world's population. The lives of people in East Asia are deeply affected by the East Asian summer monsoon (EASM) and the relationship between dust aerosols and the EASM is of great interest to the scientific community. Simulations have shown that dust aerosols not only weaken the EASM (Sun et al., 2012; Guo and Yin, 2015), but can also reduce the atmospheric heat source over the Tibetan Plateau (TP) and delay the onset of the EASM (Sun et al., 2016). Aerosols, including dust aerosols, have been shown to affect the intensity of the EASM (Li et al., 2016) and variations in the EASM can modulate the spatiotemporal distribution of dust aerosols in East Asia. A recent modeling study by Lou et al. (2016) indicated that there was a negative correlation between the spring dust loading in eastern China and the East Asian monsoon.

Dust aerosols in East Asia are mainly derived from arid and semi-arid areas, including the Taklimakan Desert and the Gobi Desert. However, some studies have indicated that the TP itself may also be an important source region for dust (Zhang et al., 1996; Fang et al., 1999) and that the region is more conducive to the atmospheric transportation of dust due to its high altitude and it can interact directly with the TP thermal pump (Wu et al., 2012). However, the source and spatiotemporal distribution of dust aerosols over the TP have not been established yet. At present, there are three viewpoints about the source of dust aerosols over the TP. First, an investigation by Fang et al. (1995, 1999) showed that there exists 2047.41×10^4 km^2 of desert land over the TP, suggesting that the TP may be a potential source for dust. A numerical simulation by Chen et al. (2013) showed that dust aerosols were produced by local emissions over the TP in spring and winter. Second, satellite observations have shown that the aerosols over the TP are dominated by dust in spring and summer and that the dust aerosols were probably derived from the Taklimakan Desert and the Gurbantunggut Desert to the north of the TP (Huang et al., 2007; Jia et al., 2015). Third, some studies have indicated that the dust emitted from the south of the TP, such as from the Great Indian Desert, can also be transported over the Himalaya (Lau et al., 2006, 2010).

As a massive, elevated heat source, the TP can directly heat the upper troposphere. The heating anomaly over the TP has a great impact on the EASM (Yanai and Wu, 2006; Duan et al., 2012). Studies have shown that dust aerosols over the TP can alter the local atmospheric radiation balance, affecting both the heat source over the TP and the Asian monsoon (Lau et al., 2006, 2010; Chen et al., 2013; Sun et al., 2016). However, most previous simulation studies have focused on dust aerosols originating from the Taklimakan and Gobi deserts (Zhao et al., 2006; Wang et al., 2008; Huang et al., 2009; Sun et al., 2012) and there have been few investigations of the impact of dust aerosols emitted by the TP on the East

Asian climate. The work reported here used the RegCM4.1 model to simulate climatic effects of distribution of dust aerosols surrounding the TP by performing numerical experiments with and without the emission of dust over the TP.

2 Numerical model and experiment design

2.1 RegCM4.1 model

5   We used the RegCM4.1 model (Regional Climate Model version 4.1), which is developed and supported by the National Center for Atmospheric Research (NCAR) and the International Center for Theoretical Physics. The model has been widely used for more than 20 years in studies of regional climatic and environmental change, especially in the simulation of the effect of aerosols on climate (Qian et al., 2003; Solomon et al., 2008; Zhang et al., 2009; Zanis et al., 2012; Ji et al., 2011, 2015; Das et al., 2015a, 2016; Mbienda et al., 2017).

10   The dynamic framework of RegCM4.1 core is based on the hydrostatic core of the mesoscale model MM5 (Grell et al., 1994). The radiation scheme in RegCM4.1 is the CCM3 radiation transfer process (Kiehl et al., 1996). RegCM4.1 has two land surface process schemes: (1) the biosphere atmosphere transfer scheme (BATS1e) (Dickinson et al., 1993); and (2) the Common Land Surface process module (CLM3.5) (Oleson et al., 2008). The dust cycle can only be diagnosed when BATS1e is used. The planetary boundary layer parameterization in RegCM4.1 follows the scheme of Holtslag et al. (1990)

15 and there are three cumulus convection parameterization schemes, including Grell (Grell et al., 1993), Kuo (Anthes, 1977) and MIT-Emmanuel (Emanuel, 1991). The dust module coupled in RegCM4.1 is based on the dust emission model (DPM) of Marticorena et al. (1995) and Alfaro and Gomes (2001). It considers dust emission, dry/wet deposition and the diagnosis of the optical and radiation characteristics of dust (including long- and short-wave radiation) (Zakey et al., 2006; Zhang et al., 2009). RegCM4.1 uses the δ-Eddington approximation for radiative flux calculations and the calculation of

20 dust short-wave radiation uses an asymmetry factor, single scattering albedo and mass extinction coefficient based on the Mie theory. The dust long-wave radiation is accounted for by introducing the dust emissivity given by Kiehl et al. (1996).

    The coupled dust module has been described in detail in previous articles (Zakey et al., 2006; Zhang et al., 2009); so only a brief introduction is given here. There are four steps in dust parameterization. First, each model grid cell is classified as either desert or non-desert according to its soil properties (such as texture, soil type, particle size and

25 composition) based on the United States Department of Agriculture textural classification. Second, dust emission is assumed to be a function of friction velocity (u^*); dust aerosols is lifted off the ground once u^* exceeds a threshold value ($u_t^*(D_p)$).

$$u_t^*(D_p) = u_{ts}^*(D_p) \cdot f_{eff} \cdot f_w, \tag{1}$$

there $u_{ts}^*(D_p)$ depends on soil particle size(D_p), f_{eff} and f_w are the correction terms for nonerodible surface roughness

30 elements (Marticorena and Bergametti, 1995) and soil moisture content (Fecan et al., 1999), respectively.

Third, the horizontal mass flux is treated as a function of the frictional velocity and is given by:

$$dH_F(D_p) = E \cdot \frac{\rho_a}{g} \cdot u^{*3} \cdot (1 + R(D_p)) \cdot (1 - R^2(D_p)) \cdot dS_{rel}(D_p),$$ (2)

where E, ρ_a and g are the ratio of the erodible to total surface areas, the surface air density and the gravitational acceleration, respectively. $R(D_p)$ is the ratio of the threshold frictional velocity in equation (1) to the frictional velocity u^* calculated within each grid cell from the model prognostic surface wind and surface roughness height. $dS_{rel}(D_p)$ is the relative surface area of a soil aggregate of diameter D_p to the total surface area of soil aggregates. The vertical flux corresponding to each emission mode is calculated by:

$$F_{dust,i}(D_p) = (\frac{\pi}{6}) \cdot \rho_p \cdot D_i^3 \cdot N_i,$$ (3)

where ρ_p is the aggregate density (2.65 g cm^{-3}), D_i is the median diameter and N_i is a function of the kinetic energy flux.

The dust particles are divided into four size bins (or modes): fine (0.01–1.0 μm), accumulation (1.0–2.5 μm), coarse (2.5–5 μm) and giant (5.0–20.0 μm). The dust transport, deposition and removal processes are given by Qian et al. (2001) and Qian and Giorgi (1999):

$$\frac{\partial \chi^i}{\partial t} = -\overline{V} \cdot \nabla \chi^i + F_H^i + F_V^i + F_C^i + S^i - R_{Wls}^i - R_{Wc}^i - D_d^i,$$ (4)

where χ is the dust mixing ratio, $\overline{V}$ is vector wind, and $-\overline{V} \cdot \nabla \chi^i$ is the advection, F_H^i is the horizontal turbulent diffusion, F_V^i is the vertical turbulent diffusion and F_C^i is the convective transport. R_{Wls}^i and R_{Wc}^i are the wet removal terms, represented by large-scale and convective precipitation. D_d^i is the dry deposition, represented by assuming fixed depositional velocities over both land and water.

2.2 Experimental design and observational data

Two numerical experiments were designed; both integrate for 20 years (excluding first two years of spin-up) using the dust-coupled RegCM4.1. The first experiment was a control experiment (CON) that used the default land use types from the Global Land Cover Characterization dataset (Loveland et al., 2000), meaning that dust emitting sources both within and outside the TP. The second experiment was a sensitivity experiment (SEN) where we turned off the dust emission in the northern and northeastern TP (the deserts inside the black outline of the TP contour in Fig. 1b). To eliminate the dust emission in the TP, we replaced the land cover types of these areas with the nearby vegetated types, in a manner similar to the method of Liu et al., (2015a). All the other conditions in the sensitivity experiment were the same as in the control experiment. In order to isolate the effect of dust aerosols, only dust aerosols are included in our simulations, without considering other aerosols (such as anthropogenic or marine aerosols).

The initial and boundary conditions were taken from the NCAR/NCEP re-analysis dataset (Kalnay et al., 1996). The sea surface temperature used the National Oceanic and Atmospheric Administration sea surface temperature dataset (Reynolds et al., 2002). The topography of the TP is very complex, necessitating high spatial resolution (<60 km) to resolve localized precipitation (Gao et al., 2006). The horizontal resolution in RegCM4.1 runs was therefore set to 40 km.

5 The simulation domain is shown in Fig. 1a and the model domain centered was at (32°N, 105°E), with 240 grid cells in the west–east direction and 160 grid cells in the north–south direction, respectively. The model was run in the standard configuration of 18 vertical σ layers with the model top at 10 hPa. The integration duration for both experiments was from January 1, 1988 to December 31, 2009. The first two years were treated as the model spin-up time and only the results from the last 20 years were analyzed.

10 **Five** main types of observations were used to evaluate the simulated results of CON: (1) the monthly mean surface air temperature and precipitation, with a high resolution of 0.5×0.5°, provided by the Climate Research Unit (CRU) of the University of East Anglia (Mitchell and Jones, 2005), which was used to evaluate the simulated surface temperature and precipitation in CON; (2) the NCEP–DOE re-analysis wind field (2.5×2.5°) at 850 hPa, which was used to compare the simulated atmospheric circulation; (3) level-3 monthly mean AOD data during 2000 to 2009 obtained from the Multiangle

15 Imaging Spectroradiometer (MISR) onboard NASA's Earth Observation System Terra satellite (http://www-misr.jpl.nasa.gov/). Since MODIS AOD has a large portion of missing data in Northwest China, MISR was used to evaluate the simulated dust AOD in CON. The effectiveness of the MISR data was investigated by Martonchik et al. (1998, 2004) and Bibi et al. (2015). (4) level-3 monthly mean pure dust AOD data under cloud free scenes (2×5°) from 2007 to 2009 obtained from Cloud-Aerosol Lidar and Infrared Pathfinder Satellite Observations (CALIPSO) (Winker et

20 al., 2013), which was also used to evaluated the simulated dust AOD in CON. The most recent version of the L3 product included averaging of individual types (Liu et al., 2008; Amiridis et al., 2013; Marinou et al., 2016); and (5) the AOD observed *in situ* by the Aerosol Robotic Network (AERONET), which was used to evaluate the simulated dust seasonal and interannual variation in CON.

3 Results of simulations

25 In this section we will first evaluate the CON simulation using the observed data described in the previous section. Then the results from CON and SEN experiments will be compared to determine the roles of dust aerosols generated from the TP play in the thermodynamic fields and circulations including the EASM.

3.1 Validation

3.1.1 Basic model climatology

30 The simulated climatology can influence the distribution of dust aerosols and their climatic effects, so CON was used to analyze the surface temperature, precipitation and atmospheric circulation at 850 hPa. The CON-simulated and CRU-

observed 20-year average summer surface temperatures in East Asia are presented respectively in Figs 2a and 2b. The CRU observed temperature is >25°C in southern China, NW China and northern India, and <7°C over the TP. The observed north–south gradient and location of the maximum and minimum centers were captured well by RegCM4.1. The model captured the major distribution patterns of precipitation, including the reasonable SE–NW gradient and the maximum centers in southern China, the Himalaya and Indian Peninsula, with a 2–4 mmday^{-1} negative bias in the Korean Peninsula and south Japan and a 2–4 mmday^{-1} positive bias in the Tianshan Mountains (Figs. 2c, 2d). These simulated deviations are likely related to the cumulus convective scheme in the model (Zhang et al., 2008; Wang and Yu, 2011). RegCM4.1 captured the major characteristics of the circulations in East Asia, where southwesterlies dominate to the south side of the TP, and the location of the Indian Low is consistent with the NCEP–DOE observations (Figs. 2e, 2f).

3.1.2 Dust AOD comparison between simulated and MISR observed

Satellite and *in situ* observations include all types of aerosols, such as black aerosols, SO_2 and organic carbon; observed data for dust AOD alone are scarce. Therefore we used the MISR AOD data, as in most previous studies (Zakey et al., 2006; Zhang et al., 2009), to evaluate the spatiotemporal distribution of the dust AOD simulated by the model. Both the simulation and observations showed that the dust AOD over the TP and its surrounding areas was higher in spring and summer (Figs. 3a and 3c) and lower in autumn and winter (Figs. 3e and 3g). There were three maximum centers (maximum value >0.6) of dust AOD in spring and summer, located in the Taklimakan Desert, the Gobi Desert and the Great Indian Desert, **respectively**. The dust AOD over the Qaidam Basin in the NE of the TP was also >0.5 and the dust AOD over the northern TP, adjacent to the southern Taklimakan Desert, was between 0.3 and 0.5. The simulated dust AOD in these regions was reduced in autumn and winter (Figs. 3e and 3g). The MISR-observed AOD was largely consistent with the model results for the Taklimakan Desert, the Gobi Desert and the Qaidam Basin, but were relatively low in the Great Indian Desert in summer. The large value of the MISR AOD in the Sichuan Basin to the east of the TP was due to industrial emissions, which were not incorporated into our model simulation.

3.1.3 Dust AOD comparison between simulated and AERONET-observed

Figure 4 compares the *in situ* observed monthly mean AOD from AERONET and that simulated by RegCM4.1 at Dalanzadgad (43.6°N, 104.4°E). This is the only available AERONET site in the vicinity of the dust sources with continuous records for >10 years. The model captured the seasonal and interannual variations of AOD well, including the year with extremely high levels of dust. Observations over the TP are scarce and we could only find a site with continuous aerosol records from AERONET at Nam Co (30.77°N, 90.96°E). The seasonal variation of AOD at this site is well captured. Both the simulation and the observations showed that the dust AOD increases in spring at Nam Co (Fig. 5).

3.1.4 Simulated and CALIPSO-observed dust AOD comparison

While MISR and AERONET data contain all types aerosols including those anthropogenic ones, the CALIPSO observation sole devotes to dust aerosols. Figure 6 shows that the simulated seasonal variation, center positions and magnitude of dust AOD are very consistent with those observed by CALIPSO during day and night. Both simulations and observations not only showed that dust AOD increased in spring and summer and decreased in autumn and winter, but also captured three maximum centers of dust AOD in Taklimakan, the Great Indian Desert and Qaidam Basin located in the northern TP in spring. The simulated center values were still high in summer. Besides, it is very interesting to note that the observed dust AOD in the Qaidam Basin is higher at night than that during daytime (Figure 6b and 6c), which implies that dust activities in the TP may be more prominent at night. This unusual feature could cause dust radiative effects in the TP is very different from those of in other locations, which is further discussed in the subsequent section of 3.4.1

3.2 Relationship between the EASM and dust loading over the TP

To study the relationship between dust aerosols and the EASM, we used the average summer meridional wind at 850 hPa over eastern China (20–45°N, 105–122.5°E) as an EASM index, following Xie et al. (2016). This index measures the intensity of the southerly wind to the east of TP in lower troposphere above East Asia. It has been widely used to examine both modern and paleo-changes in the East Asian monsoon (Wang et al., 2008; Jiang and Lang, 2010). We found that the simulated difference in the EASM index (CON−SEN) and the difference in the model-simulated column dust load averaged over the TP are highly anticorrelated with a correlation coefficient $R=-0.41$ (Fig. 7). The dust aerosol increases and decreases over the TP as the index weakens and enhances respectively. Lou et al. (2016) also demonstrated a clear negative correlation between the EASM and the dust concentration over eastern China in spring. Based on the variation in the column dust load shown in Fig. 7, we chose 1994 and 2009 as heavy dust years and 2003 and 2007 as light dust years and then contrasted the dust distribution over the TP and its effects on the summer climate in the heavy/light dust years.

3.3 Dust aerosol distribution in heavy/light dust years

In the heavy dust years, the difference in the column dust load over the TP was greater than that in the light dust years, as expected. Two centers of maximum column dust load existed over the TP in the heavy dust years (Fig. 8a). One was located in the Qaidam Basin and the other in the NW of the TP. The maximum values at both centers were >70 mg m^{-2}. However, the difference in the column dust load over the NW of the TP in the light dust years was much lower than in the heavy dust years and the central value was <25 mg m^{-2}. From the vertical profiles of the dust load (Figs 8c and 8d), we can see that the dust mixing ratio was higher in heavy dust years in the western TP with a central value >5 μg kg^{-1}. The mixing ratio was lower in the western TP in the light dust years.

3.4 East Asian climate anomalies in heavy/light dust years induced by dust aerosols

3.4.1 Temperature anomaly

Both the atmospheric heating rate and the atmospheric temperature over the TP decreased in heavy/light dust years (Fig. 9). During the heavy dust years, the dust aerosol resulted in two cooling anomaly centers, one in the lower troposphere (600–400 hPa) over TP core and the other in the upper troposphere (*c.* 300 hPa) of the western TP, with a cooling of >0.4 K day^{-1} due to the large dust load. These cooling anomalies resulted in a low temperature center at 500 hPa over the western TP, with its central value reduced by >0.6°C. The dust aerosol over the TP in the light dust years was much less than in the heavy dust years (Fig. 8a and 8c), so the cooling effect in the light dust years was weaker than in the heavy dust years. The warming to the east of the TP (110–120°E) (Fig. 9c and 9d) is caused by diabatic heating induced by the enhancement of descending motion. The enhanced descending motion was induced by the LW cooling effects of dust over the TP (figures not shown).

The surface temperature over the TP decreased in both the heavy and light dust years (Fig. 10). In the heavy dust years, the surface temperature decreased by 0.6°C over the TP and the sea–land thermal contrast was reduced. It is worth noting that the effects of TP aerosols on surface temperature were not limited to local or surrounding regions. In fact, the largest impact was in NE China, more than two thousands km downstream (Fig. 10a). The remote cooling is likely contributable to a cold air advection stemmed from the upstream TP aerosols to be discussed in next subsection (Fig. 11). Similar phenomena were reported earlier from Europe for anthropogenic aerosols (Zanis 2009; Zanis et al., 2012) and from South Asia for natural aerosols (Das et al., 2015a).

3.4.2 Circulation

The overall effects of TP aerosols cool the troposphere surrounding the TP (Fig. 10a) and thus the land–sea thermal contrast was reduced by the dust aerosols over the TP. The atmospheric circulation anomaly induced by the dust aerosols emitted over the TP in heavy dust years shows an overall gigantic anticyclonic circulation centered over the TP with a positive anomaly (>10m) in geopotential height (Fig. 11a). The northeasterlies that run against the southwesterly monsoon is especially strong over the EASM region, which indicates that the EASM was weakened greatly. The anomaly still existed in the light dust years, but its intensity was much weaker than in the heavy dust years (Fig. 11b).

3.4.3 Precipitation

Figure 12 shows the simulated change in summer precipitation in East Asia induced by dust emitted over the TP in heavy and light dust years. The precipitation decreased in both the southern and the northern monsoon regions in summer in the heavy dust years as a result of weakening of the EASM (Fig. 11), and the reduction in the southern monsoon region is greater than that in the northern monsoon region. The dust aerosols also reduced precipitation in the two monsoon regions in the light dust years. The simulated suppressive effects of the dust aerosols were consistent with previously

reported modeling results (Sun et al., 2012; Guo et al., 2015). Besides, precipitation in the heavy dust years reduced more than that in the light dust years in the TP, which may be suppressed by the enhancement of descending motion induced by the strong cooling effects of dust aerosol over the TP.

4 Discussion

5   Previous research has shown that dust emitted from Asian deserts can weaken the EASM (Sun et al., 2012; Guo et al., 2015; Li et al., 2016), although the details of weakening mechanisms are still unclear. It has been suggested by some authors that the weakening of the EASM is a result of the reduction in the thermal contrast between the land and the sea induced by dust aerosols (Guo and Yin, 2015; Li et al., 2016). However, the modeling result of Sun et al. (2012) showed that the EASM is reduced by the large-scale atmospheric disturbances (cyclone–anticyclone–cyclone Rossby wave train)

10 generated by the radiative cooling of dust aerosols. In the work reported here, we considered the effects of dust aerosols emitted only within the TP itself on regional climate and found that they can also reduce the EASM significantly by weakening the heat source ("pump") over the TP and thus reduce the land–sea thermal contrast. The locally generated TP dust can cause surface cooling far downstream in eastern Mongolia and northeastern China through stationary Rossby wave propagation. The dust-loading over the TP include both local emissions and external sources; our sensitivity

15 simulations showed there was a negative correlation between the EASM and dust aerosols emitted from the TP locally.

     The spring dust aerosols from the TP have a close relation with EASM. Although the cause-effect relationship is not immediately clear, the following processes are proposed as a possible mechanism of this relation based on the results in our simulation (Fig. 13). Firstly, increasing (decreasing) in dust aerosol over the TP in the heavy (light) dust years in spring can weaken (enhance) the TP heat source and thus reduce (increase) precipitation over the TP. Reduction (increase)

20 in precipitation over the TP can also further enhance (diminish) dust emission over the TP. Secondly, the weakened (enhanced) TP heat source can persist from spring to summer and shrink (expand) the land-sea thermal contrast and thus weaken (enhance) the EASM. Therefore, the change of dust over the TP has an anti-correlation with the variation of EASM circulation intensity. Thirdly, weakened (enhanced) monsoon circulation can reduce (increase) precipitation in East Asia. As a result, the precipitation variation of the TP presents a positive-correlation with that of EASM.

25   It is worth noting that Sun and Liu (2016) demonstrated that dust emitted from Taklimakan and Gobi Deserts weakens the Asian monsoon through large-scale atmospheric disturbances by 2 m s^{-1} of wind at 700 hPa. This magnitude of reduction in the wind seems small compared to the values in the present study even though the emission source extent in the previous is larger. We think both high-altitude source like the TP and low-altitude sources such as Taklimakan and Gobi Desert can weaken the EASM, but the mechanism could differ. The dust emitted from low altitude source (mainly

30 Taklimakan and Gobi Desert) reduces the EASM mainly by the large-scale atmospheric disturbances, while the dust emitted from high-altitude source weakens the EASM by the reduction in the TP heating and in thermal contrast in the middle troposphere between the land and sea. The column dust load induced by local emissions from the TP in heavy dust

years accounted for 20% ((CON−SEN)/CON) of the total loading over the TP, its impacts on Asian monsoon and climate seems more important than the low altitude sources such as Taklimakan and Gobi Desert in East Asia. This disproportionately large impact from TP locally emitted dust is likely due to its higher elevation within TP itself so that the dust-induced cooling can more effectively weaken the TP's acting as a heat pump for the Asian monsoon. Further
5 studies on this is rightly warranted.

Dust direct radiative effects is reported predominantly positive (warming) over land areas in most of previous researches (Zhang et al., 2013; Chen et al., 2013), but it can become negative under specific situations like a large zenith angle (Quijano et al., 2000). It is interesting to note that it can also become negative when dust activities are mainly vigorous at night over the TP. The observed dust AOD at night is much higher than those of during daytime over the TP
10 (Figure 6b and 6c); so the SW warming effects is quite weaker than the LW cooling effects (figures not shown). The simulations of Chen et al. (2013) included strong absorbing aerosols such as black carbon and included contribution of other dust sources including such as the Taklimakan and the Gurbantunggut Desert to the north of the TP and that from the Great Indian Desert to the south of the TP; thus, the warming effects of dust aerosol reported in their study is broader. In contrast, the cooling effects in our study is mainly caused by the dust aerosol emitted from the TP at night.

15 It is worth mentioning that the model's internal variability could influence the results; so we compared the standard deviation of summer surface temperature and precipitation in CON with the signal induced by the dust effects (CON minus SEN) during the heavy dust years. The signal induced by the dust is much greater than the standard deviations (figures not shown). Therefore, the dust effect reported in our simulation is significant in the heavy dust years, but the cooling over central India in the light dust years may be caused by the model's internal variability. Besides, the results
20 could also include the role of changed land cover in addition to the role of dust aerosols because turning off dust emission in the TP was through modifying underlying surface types. Hence, we carried out two additional sensitive experiments to isolate effects of the changed land cover alone. The dust cycle in the two experiments was turned off, but the land cover was changed to one similar to the modification in SEN. The differences between them only included effects of the changed land cover. The results showed that the change (from desert to vegetated land) brought about 0.4 °C warming
25 (figures not shown), and this warming effects is weaker than the combined cooling effects (–0.6°C) induced by the dust aerosol and the changed land cover together. Besides, it is interesting to note that Li and Xue (2010) demonstrated that the land cover change from vegetated land to bare ground (mainly desert) in the TP decreased the radiation absorbed by the surface and resulted in weaker surface thermal effects, which means that the effect of land cover change from desert to vegetated land may also cause warming effects. This is opposite to the cooling effect induced by the dust aerosols over the
30 TP in our simulation, and the warming may partly offset the dust aerosols-induced cooling effect. However, our results showed that the signal of cooling effects was not changed, although it may even be underestimated. Therefore, actual cooling should be stronger than the simulated value. Hence, the reported dust effects also need be evaluated by using a refined way in the future.

It is very beneficial to study the impact of aerosols on climate using a RCM instead of a coarse-resolution global climate model (GCM). The GCMs tend to systematically underestimated dust aerosol concentration, presumably due to their lower spatial resolution (Tegen et al., 2002; Zhang et al., 2009). The RCM simulated dust concentration, on the other hand, was closer to the observed magnitude compared with the results of global models (Sun et al., 2012). For example,

5   previous studies showed that high-resolution RCMs had better capabilities than GCMs in simulating the effect of aerosols on Asian monsoon (Zhou and Yu, 2006; Gao et al., 2008; Ji et al., 2011). A high-resolution regional model is especially needed to capture subtle characteristics in the areas of complex terrain (Ji et al., 2011). However, limited area RCM naturally cannot fully account for external forcing remote from the domain of interest although the lateral boundary conditions allow large-scale features to propagate into the domain. Our domain size (9600 km × 640 km) is reasonably

10   large enough so that the weather and climate systems can have adequate spatial extent to develop within the domain, as attested by reasonably validation of wind pattern, temperature field, and precipitation (Section 3.1). Cautions should be exercised, however, that results from regional simulations could be somewhat domain-size dependent quantitatively although main results should not be affected.

Only direct radiative effects of dust were included in our model and future studies should include both direct and

15   indirect effects. The simulated effects of dust aerosols on climate were highly sensitive to the physical characteristics of the dust aerosols, such as the single scattering albedo (Huang et al., 2014; Colarco et al., 2014; Das et al., 2015b). Therefore our results also need to be validated by sensitivity experiments using aerosols with different properties. A recent study by Tsikerdekis et al. (2017) demonstrated that simulated dust load and induced radiation change are sensitive to the dust particle size division in the model; so further sensitivity experiments using more dust size bins would be

20   worthwhile. In addition, many other factors can also affect the EASM, including the El Niño Southern Oscillation (Zhao et al., 2012; Liu et al., 2015b), the North Atlantic Oscillation (Wu et al., 2009) and heat sources over the TP (Yanai and Wu, 2006; Duan et al., 2012). A recent numerical simulation by Wang et al. (2017) showed that aerosol emissions from outside East Asian play an important part in weakening the circulation of the EASM.

5 Conclusions

25   We conducted two numerical experiments to quantify the effects of dust aerosols emitted over the TP on the EASM in heavy/light dust years using a high-resolution regional climate model. Satellite and *in situ* observations were used to evaluate the simulated spatial distribution of dust aerosols and their seasonal and interannual variations. We analyzed the change in dust aerosols induced by emissions over the TP and their radiative effects on the EASM and summer precipitation in heavy/light dust years. We also studied the effects of dust aerosols on the onset of the EASM.

30   The spatiotemporal distribution of the dust AOD and their seasonal and interannual variation were captured well by the RegCM4.1 model compared with the MISR AOD and *in situ* observations from AERONET. Both the simulated and observed AOD were higher in spring/summer and lower in autumn/winter. The simulated dust AOD was higher in the

Taklimakan Desert, the Gobi Desert and the Great Indian Desert, with peak values >0.6. The simulated dust AOD in the Qaidam Basin and the northern TP were also higher. The seasonal variation in the dust AOD at Nam Co was captured well by RegCM4.1 relative to the observed aerosol AOD.

Comparative analyses of the two simulations indicated that the dust aerosols generated over the TP had a profound influence on the EASM. The difference in the EASM index and column dust load between CON and SEN experiments are negatively correlated ($r=-0.41$). The index also weakened (enhanced) as the imported-local combined dust aerosol increased (decreased) over the TP. The net atmospheric heating rate was negative over the TP in heavy dust years as a result of the radiative cooling effects of the dust aerosols, leading to a 0.6°C cooling in the surface and atmospheric temperatures. The land–sea thermal contrast and EASM were therefore both weakened, causing a 12% reduction in precipitation in the southern monsoon region. The dust load over the TP in the light dust years was much less than in the heavy dust years, implying large interannual variability. The dust aerosols produced over the TP can delay the onset of the EASM by one pentad in both the northern and southern monsoon regions of China.

Acknowledgements. The authors thank the two anonymous reviewers for valuable comments and suggestions. This research was jointly supported by the National Key Research and Development Program of China (2016YFA0601904), the National Natural Science Foundation of China (41405093, 41572150, and 41475085).

References

Alfaro, S. C. and Gomes, L.: Modeling mineral aerosol production by wind erosion: Emission intensities and aerosol size distributions in source areas, J. Geophys. Res., 106(D16), 18075–18084, doi:10.1029/2000JD900339, 2001.

Amiridis, V., Wandinger, U. Marinou, E. Giannakaki, E., Tsekeri, A., Basart, S., Kazadzis, S., Gkikas, A., Taylor, M., Baldasano, J., Ansmann, A.: Optimizing CALIPSO Saharan dust retrievals, Atmos. Chem. Phys., 13, 12089–12106, doi: 10.5194/acp-13-12089-2013, 2013.

Anthes, R. A.: A cumulus parameterization scheme utilizing a one-dimensional cloud model, Mon. Weather Rev., 105, 270–286, doi: http://dx.doi.org/10.1175/1520-0493(1977)105<0270:ACPSUA>2.0.CO;2, 1977.

Bibi, H., Alam, K., Chishtie, F., Bibi. S., Shahid, I., and Blaschke, T.: Intercomparison of MODIS, MISR, OMI, and CALIPSO aerosol optical depth retrievals for four locations on the Indo-Gangetic plains and validation against AERONET data, Atmos. Environ., 111, 113–126, 2015.

Chen, S. Y., Huang, J. P., Zhao, C., Qian, Y., Leung, R., and Yang, B.: Modeling the transport and radiative forcing of Taklimakan dust over the Tibetan Plateau: A case study in the summer of 2006, J. Geophys. Res., 118, 797–812, doi: 10.1002/jgrd.50122, 2013.

Colarco, P. R., Nowottnick, E. P., Randles, C. A., Yi, B. Q., Yang, P., Kim, K. M., Smith, J. A., and Bardeen, C. G.: Impact of radiatively interactive dust aerosols in the NASA GEOS-5 climate model: sensitivity to dust particle shape and refractive index, J. Geophys. Res., 119(2), 753–786, doi: 10.1002/2013JD020046, 2014.

Das, S., Dey, S., and Dash, S. K.: Impacts of aerosols on dynamics of Indian summer monsoon using a regional climate model, Clim. Dyn., 44, 1685–1697, doi:10.1007/s00382-014-2284-4, 2015a.

Das, S., Dey, S., Dash, S. K., Giuliani, G., and Solmon, F.: Dust aerosol feedback on the Indian summer monsoon: Sensitivity to absorption property, J. Geophys. Res., 120, 9642–9652, doi: 10.1002/2015JD023589, 2015b.

Das, S., Dey, S., Dash, and S. K.: Direct radiative effects of anthropogenic aerosols on Indian summer monsoon circulation, Theor. Appl. Climatol. 124, 629–639, doi: 10.1007/s00704-015-1444-8, 2016.

Dickinson, R. E., Henderson-Sellers, A., and Kennedy, P. J.: Biosphere-atmosphere transfer scheme (bats) version 1e as coupled to the NCAR community climate model, NCAR Tech., National Center for Atmospheric Research Technical Note No. TN-387+STR, NCAR, Boulder, CO, 1993.

Duan, A., Wu, G., Liu, Y., Ma, Y., and Zhao, P.: Weather and climate effects of the Tibetan Plateau, Adv. Atmos. Sci., 29, 78–992, doi: 10.1007/s00376-012-1220-y, 2012.

Emanuel, K. A.: A scheme for representing cumulus convection in large-scale models, J. Atmos. Sci., 48(21), 2313–2335, doi: 10.1175/1520-0469(1991)048<2313:ASFRCC>2.0.CO;2, 1991.

Fang, X. M.: The origin and provenance of the Malan loess along the eastern margin of the Qinhai-Xizang (Tibetan) Plateau and its adjacent area, Sci. China SER B, 38(7), 876–887, 1995.

Fang, X. M., Li, J. J., and Van der Voo, R.: Rock magnetic and grain size evidence for intensified Asian atmospheric circulation since 800 kyrs BP to Tibetan uplift. Earth Planet, Sc. Lett., 165, 129–144, doi: http://dx.doi.org/10.1016/S0012-821X(98)00259-3, 1999.

Fecan, F., Marticorena, B., and Bergametti, G.: Parameterization of the increase of aeolian erosion threshold wind friction velocity due to soil moisture for arid and semi-arid areas, Ann. Geophys., 17, 149–157, doi: 10.1007/s00585-999-0149-7, 1999.

Gao, X. J., Xu, Y., Zhao, Z. C, Pal, J. S., and Giorgi, F.: On the role of resolution and topography in the simulation of East Asia precipitation, Theor. Appl. Climatol., 86, 173–185, doi: 10.1007/s00704-005-0214-4, 2006.

Gao, X. J., Shi, Y., Song, R., Giorgi, F., Wang, Y., and Zhang, D.: Reduction of future monsoon precipitation over China: comparison between a high resolution RCM simulation and the driving GCM, Meteor Atmos. Phys., 100, 73–86, 2008.

Giorgi. F., Coppola, E., Solmon, F., Mariotti, L., Sylla, M. B., Bi, X., Elguindi, N., Diro, G. T., Nair, V., Giuliani, G., Turuncoglu, U. U., Cozzini, S., Güttler, I., O'Brien, T. A., Tawfik, A. B., Shalaby., Zakey, A. S., Steiner, A. L., Stordal, F., Sloan, L. C., and Brankovic, C.: RegCM4: Model description and preliminary tests over multiple CORDEX domains, Clim. Res., 52, 7–29, doi: 10.3354/cr01018, 2012.

Goudie, A. S.: Dust storms in space and time, Prog. Phys. Geog., 7, 502–530, doi: 10.1177/030913338300700402, 1983.

Grell, G. A., Dudhia, J., and Stauffer, D. R.: Description of the fifth generation Penn State/NCAR Mesoscale Model (MM5), National Center for Atmospheric Research Technical Note No. TN-398+STR, NCAR, Boulder, Colo, 1994.

Grell, G. A.: Prognostic evaluation of assumptions used by cumulu parameterizations, Mon. Weather Rev., 121, 764–787, doi: 10.1175/1520-0493(1993)121<0764:PEOAUB>2.0.CO;2, 1993.

5 Guo, J. and Yin, Y.: Mineral dust impacts on regional precipitation and summer circulation in East Asia using a regional coupled climate system model, J. Geophys. Res., 120, 10378–10398, doi: 10.1002/2015JD023096, 2015.

Holtslag, A., De Bruijn, E., and Pan, H. L.: A high resolution air mass transformation model for short-range weather forecasting, Mon. Weather Rev., 118(8), 1561–1575, doi: 10.1175/1520-0493(1990)118<1561:AHRAMT>2.0.CO;2, 1990.

10 Huang, J. P., Minnis, P., Yi, Y. H., Tang, Q., Wang, X., Hu, Y. X., Liu, Z. Y., Ayers, K., Trepte, C., and Winker, D.: Summer dust aerosols detected from CALIPSO over the Tibetan Plateau, Geophys. Res. Lett., 34, L18805, doi:10.1029/2007GL029938, 2007.

Huang, J. P., Fu, Q., Su, J., Tang, Q., Minnis, P., Hu, Y., Yi, Y., and Zhao Q.: Taklimakan dust aerosol radiative heating derived from CALIPSO observations using the Fu-Liou radiation model with CERES constraints, Atmos. Chem.
15   Phys., 9, 4011–4021, doi: 10.5194/acp-9-4011-2009, 2009.

Huang, J. P., Wang, T., Wang, W., Li, Z., and Yan, H.: Climate effects of dust aerosols over East Asian arid and semiarid regions, J. Geophys. Res., 110, 11398–11416, doi: 10.1002/2014JD021796, 2014.

Ji, Z. M., Kang, S. C., Zhang, D. F., Zhu, C. Z., Wu, J., and Xu, Y.: Simulation of the anthropogenic aerosols over South Asia and their effects on Indian summer monsoon, Clim. Dyn., 36, 1633–1647, doi: 10.1007/s00382-010-0982-0,
20   2011.

Ji, Z. M., Kang, S. C., Cong, Z. Y., Zhang, Q. G., and Yao, T. D.: Simulation of carbonaceous aerosols over the Third Pole and adjacent regions: distribution, transportation, deposition, and climatic effects, Clim. Dyn., 45, 2831–2846, doi: 10.1007/s00382-015-2509-1, 2015.

Jia, R., Liu, Y., Chen, B., Zhang, Z., and Huang, J.: Source and transportation of summer dust over the Tibetan Plateau,
25   Atmos. Environ., 123, 210–219, doi: 10.1016/j. atmosenv.2015.10.038, 2015.

Jiang, D. B. and Lang, X. M.: Last Glacial Maximum East Asian monsoon: Results of PMIP simulations, J. Clim., 23, 5030–5038, doi: 10.1175/2010JCLI3526.1, 2010.

Kalnay, E., Kanamitsu, M., Kistler, R., Collins, W. G., Deaver, D., Gandin, L. S., Iredell, M., Saha, S., White, G., Woollen, J., Zhu, Y., Chelliah, M., Ebisuzaki, W., Higgins, W., Janowiak, J. E., Mo, K., Ropelewski, C., Wang, J. L.,
30   and Leetmaa, A.: The NCEP/NCAR 40-year reanalysis project, Bull. Am. Meteorol. Soc., 77, 437–471, doi: http://dx.doi.org/10.1175/1520-0477(1996)077<0437:TNYRP>2.0.CO;2, 1996.

Kiehl, J., Hack, J., Bonan, G., Boville, B., Breigleb, B., Williamson, D., and Rasch, P.: Description of the NCAR community climate model (CCM3). National Center for Atmospheric Research Technical Note No. NACR/TN-420+STR, NCAR, Boulder, CO, 1996.

Lau, K. M., Kim, M. K, and Kim, K. M.: Asian monsoon anomalies induced by aerosol direct forcing: the role of the Tibetan Plateau, Clim. Dyn., 26, 855–64, doi: 10.1007/s00382-006-0114-z, 2006.

Lau, K. M., Kim, M. K., Kim, K. M., and Lee, W. S.: Enhanced surface warming and accelerated snow melt in the Himalayas and Tibetan Plateau induced by absorbing aerosols, Environe. Res. Lett., 5, 025204, doi: 10.1088/1748-9326/5/2/025204, 2010.

Li, S., Wang, T. J, Solmon, F., Zhuang, B. L., Wu, H., Xie, M., Han, Y., and Wang, X. M.: Impact of aerosols on regional climate in southern and northern China during strong/weak East Asian summer monsoon years, J. Geophys. Res., 121, 4069–4081, doi: 10.1002/2015JD023892, 2016.

Li, Q., and Xue Y. K.: Simulated impacts of land cover change on summer climate in the Tibetan Plateau, Envrion. Res. Lett., 5, 015102, doi: 10.1088/1748-9326/5/1/015102, 2010.

Liu, X. D. Yin, Z. Y.: Sensitivity of East Asian monsoon climate to the Tibetan Plateau, Palaeogeogr. Palaeocl., 183, 223–245, doi: 10.1016/S0031-0182(01)00488-6, 2002

Liu, D., Wang, Z., Liu, Z., Winker, D., and Trepte, C.: A height resolved global view of dust aerosols from the first year CALIPSO lidar measurements, J. Geophys. Res., 113, D16214, doi: 10.1029/2007JD009776, 2008.

Liu, X. D., Sun, H., Miao, Y. F., Dong, B. W., and Yin, Z. Y.: Impact of uplift of northern Tibetan Plateau and formation of Asian inland deserts on regional climate and environment, Quaternary Sci Rev., 116, 1–14, doi: 10.1016/j.quascirev.2015.03.010, 2015a.

Liu, Y. Y., Hu, Z. Z., Kumar, A., Peng, P., Collins, D. C., and Jha, B.: Tropospheric biennial oscillation of summer monsoon rainfall over East Asia and its association with ENSO, Clim. Dyn., 45, 1747–1759, doi: 10.1007/s00382-014-2429-5, 2015b.

Loveland, T. R., Reed, B. C., Brown, J. F., Ohlen, D. O., Zhu, Z., Yang, L., and Merchant, J. W.: Development of a global land cover characteristic database and IGBP DISCover from 1-km AVHRR data, Int. J. Remote Sens., 21(6), 1303–1330, doi: https://doi.org/10.1080/014311600210191, 2000.

Lou, S., Russell, L. M., Yang, Y., Xu, L., Lamjiri, M. A., DeFlorio, M. J., Miller, A. J., Ghan, S. J., Liu, Y., and Singh, B.: Impacts of the East Asian Monsoon on springtime dust concentrations over China, J. Geophys. Res., 121, 8137–8152, doi:10.1002/2016JD024758, 2016.

Marinou, E., Amiridis. V., Binietoglou, I. Solomos, S., Proestakis. E., Konsta, D., Tsikerdekis, A., Papagiannopoulos, N., Vlastou, G., Zanis, P., Balis, D., Wandinger, U., Ansmann, A.: 3D evolution of Saharan dust transport towards Europe based on a 9-year EARLINET-optimized CALIPSO dataset, Atmos. Chem. Phys., doi: 10.5194/acp-2016-902, 2016.

Marticorena, B. and Bergametti, G.: Modeling the atmospheric dust cycle: 1. Design of a soil-derived dust emission scheme, J. Geophys. Res., 100(D8), 16415–16430, 1995.

Martonchik, J. V., Diner, D. J., Kahn, R. A., Ackerman, T. P., Verstraete, M. E., Pinty, B., and Gordon, H. R.: Techniques for the retrieval of aerosol properties over land and ocean using multiangle imaging, IEEE Trans. Geosci. Remote Sens., 36(4), 1212–1227, 1998.

Martonchik, J. V., Diner, D. J., Kahn, R., Gaitley, B., and Holben, B. N.: Comparison of MISR and AERONET aerosol optical depths over desert sites, Geophys. Res. Lett., 31, L16102, doi: 10.1029/2004GL019807, 2004.

Mbienda, A. J. K., Tchawoua, C., Vondou, D. A., Choumbou, P., Sadem, C. K., and Dey, S.: Impact of anthropogenic aerosols on climate variability over Central Africa by using a regional climate model, Int. J. Climatol., 37, 249–267, doi: 10.1002/joc.4701, 2017.

Miller, R. L., Perlwitz, J., and Tegen, I.: Modeling Arabian dust mobilization during the Asian summer monsoon: The effect of prescribed versus calculated SST, Geophys. Res. Lett., 31(22), 519–540, doi: 10.1029/2004GL020669, 2004.

Mitchell, T. D. and Jones, P. D.: An improved method of constructing a database of monthly climate observations and associated high-resolution grids, Int. J. Climatol., 25, 693–712, doi: 10.1002/joc.1181, 2005.

Oleson, K. W., Niu, G. Y., Yang, Z. L., Lawrence, D. M., Thornton, P. E., Lawrence, P. J., Stockli, R., Dickinson, R. E., Bonan, G. B., Levis, S., Dai, A., and Qian, T.: Improvements of the Community Land Model and their impact on the Hydrological cycle, J. Geophys. Res., 113, 811–827, doi:10.1029/2007JG000563, 2008.

Park, S. S. and Kim, Y. J.: Source contributions to fine particulate matter in an urban atmosphere, Chemosphere, 59(2), 217–226, doi: 10.1013/j.chemosphere.2004.11.001, 2005.

Prasad, A. K. and Singh, R. P.: Comparison of MISR-MODIS aerosol optical depth over the Indo-Gangetic basin during the winter and summer seasons (2000–2005), Remote Sens. Environ., 107(1–2), 109–119, doi: 10.1013/j.rse.2006.09.026, 2007.

Qian, Y. and Giorgi, F.: Interactive coupling of regional climate and sulfate aerosol models over East Asia, J. Geophys. Res., 104, 6477–6499, doi:10.1029/98JD02347, 1999.

Qian, Y., Giorgi, F. Huang, Y. Chameides, W. and Luo C.: Regional simulation of anthropogenic sulfur over East Asia and its sensitivity to model parameters, Tellus B, 53, 171–191, doi:10.1034/j.1600-0889.2001.d01-14.x, 2001.

Qian, Y., Leung, L. R., Ghan, S. J., and Giorgi, F.: Regional climate effects of aerosols over China: Modeling and observation, Tellus B, 55(4), 914–934, doi: doi: 10.1046/j.1435-6935.2003.00070.x, 2003.

Quijano, A. L., Sokolik, I. N., and Toon, B.: Radiative heating rates and direct radiative forcing by mineral dust in cloudy atmospheric conditions, J. Geophys. Res., 105, 12207–12219, doi: 10.1029/2000JD900047, 2000.

Reynolds, R. W., Rayner, N. A., Smith, T. M., Stokes, D. C., and Wang, W. Q.: An improved in situ and satellite SST analysis for climate, J. Clim., 15, 1609–1625, doi: 10.1175/1520-0442(2002)015, 2002.

Rosenfeld, D., Rudich, Y., and Lahav, R.: Desert dust suppressing precipitation: A possible desertification loop, Proc. Natl. Acad. Sci. USA, 98(11), 5975–5980, doi: 10.1073/pnas.101122798, 2001

Solmon, F., Mallet, M., Elguindi, N., Giorgi, F., Zakey, A., and Konaré, A.: Dust aerosol impact on regional precipitation over western Africa, mechanisms and sensitivity to absorption properties, Geophys. Res. Lett., 35, L24705, doi: 10.1029/2008GL035900, 2008.

Sun, H., Pan, Z. T., and Liu, X. D.: Numerical simulation of spatial-temporal distribution of dust aerosol and its direct radiative effects on East Asian climate, J. Geophys. Res., 117(D13), 110–117, doi: 10.1029/2011JD017219, 2012.

Sun, H. and Liu, X. D.: Numerical modeling of topography-modulated dust aerosol distribution and its influence on the onset of East Asian summer monsoon, Adv. Meteorol., 2016(4), 1–15, doi: 10.1155/2016/6951942, 2016.

Tegen, I. and Lacis, A. A.: Modeling of particle size distribution and its influence on the radiative properties of mineral dust aerosol, J. Geophys. Res., 101(D14), 19237–19244, doi: 10.1029/95JD03610, 1996.

Tegen, I., Harrison, S. P., Kohfeld, K., Prentice, I. C., Coe, M., and Heimann M.: Impact of vegetation and preferential source areas on global dust aerosol: Results from a model study, J. Geophys. Res., 107(D21), 4576, doi:10.1029/2001JD000963, 2002.

Tsikerdekis, A., Zanis, P., Steiner, A. L., Solmon, F., Amiridis, V., Marinou, E., Katragkou, E., Karacostas, T., Foret, G.: Impact of dust size parameterizations on aerosol burden and radiative forcing in RegCM4, Atmos. Chem. Phys., 17, 769–791, doi: 10.5194/acp-17-769-2017, 2017.

Uno, I., Eguchi, K., Yumimoto, K., Takemura, T., Shimizu, A., Uematsu, M., Liu, Z., Wang, Z., Hara, Y., and Sugimoto, N.: Asian dust transported one full circuit around the globe, Nat. Geosci., 2, 557–560, doi:10.1038/ngeo583, 2009.

Wang, B. and Ho, L.: Rainy season of the Asian-Pacific summer monsoon, J. Clim., 15(4), 386–398, doi: 10.1175/1520-0442(2002)015<0386:RSOTAP>2.0.CO;2, 2002.

Wang, B., Wu, Z., Li, J., Liu, J., Chang, C. P., Ding, Y., and Wu, G.: How to measure the strength of the East Asian summer monsoon, J. Clim., 21, 4449–4463, doi: 10.1175/2008JCLI2183.1, 2008.

Wang, C. T. and Yu, L.: Sensitivity of regional climate model to different cumulus parameterization schemes in simulation of the Tibetan Plateau climate, Chin. J. Atmos. Sci., 35(6), 1132–1144 (Chinese), 2011.

Wang, Q. Y., Zhang, Z. L., and Zhang, H.: Impact of anthropogenic aerosols from global, East Asian, and non-East Asian sources on East Asian summer monsoon system, Atmos. Res., 183, 224–236, doi: 10.1016/j.atmosres.2016.08.023, 2017.

Wang, Y. Q., Zhang, X. Y., Gong, S. L., Zhou, C. H., Hu, X. Q., Liu, H. L., Niu, T., and Yang, Y. Q.: Surface observation of sand and dust storm in East Asia and its application in CUACE/Dust, Atmos. Chem. Phys., 8, 545–553, 2008.

Wu, G., Liu, Y., He, B., Bao, Q., Duan, A., and Jin, F. F.: Thermal controls on the Asian summer monsoon, Sci. Rep., 2, 404, doi: 10.1038/srep00404, 2012.

Wu, Z., Wang, B., Li, J., and Jin, F. F.: An empirical seasonal predication model of the east Asian summer monsoon using ENSO and NAO, J. Geophys. Res., 114(D18), 85–86, doi: 10.1029/2009JD011733, 2009.

Xie, X., Wang, H., Liu, X., Li, J., Wang, Z., and Liu, Y.: Distinct effects of anthropogenic aerosols on the effect Asian summer monsoon between multidecadal strong and weak monsoon stages, J. Geophys. Res., 121, doi: doi:10.1002/2015JD024228, 2016.

Yanai, M., Wu, G. X., and Wang, B.: Effects of the Tibetan Plateau In The Asian Monsoon, Springer, Berlin, 513–549, 2006.

Zakey, A. S., Solmon, F., and Giorgi, F.: Implementation and testing of a desert dust module in a regional climate model, Atmos. Chem. Phys., 6, 4687–4704, doi:10.5194/acp-6-4687-2006, 2006.

Zanis, P.: A study on the direct effect of anthropogenic aerosols on near surface air temperature over Southeastern Europe during summer 2000 based on regional climate modeling, Ann. Geo., 27, 3977–3988, 2009.

Zanis, P., Ntogras, C., Zakey, A., Pytharoulis, I., and Karacostas, T.: Regional climate feedback of anthropogenic aerosols over Europe using RegCM3, Clim. Res., 52, 267–278, doi: 10.3354/cr01070, 2012.

Zhang, X. Y., Zhang, G. Y., Zhu, G. H., Zhang, D. R., An, Z. S., and Chen, T., Huang, X. P.: Elemental tracers for Chinese source dust, Sci. China SER D, 39(5), 512–521, 1996.

Zhang, D. F., Gao, X. J., Ouyang, L. C., and Dong, W. J.: Simulation of present climate over East Asia by a regional climate model, J. Trop. Meteorol., 14, 19–23, 2008.

Zhang, D. F., Zakey, A. S, Gao, X. J., Giorgi, F., and Solmon, F.: Simulation of dust aerosol and its regional feedbacks over East Asia using a regional climate model, Atmos. Chem. Phys., 9, 1095–1110, doi:10.5194/acp-9-1095-2009, 2009.

Zhang, L., Li, Q. B., Gu, Y., Liou, K. N., and Meland, B.: Dust vertical profile impact on global radiataive forcing estimation using a coupled chemical-transport-radiative-transfer model, Atmos. Chem. Phys., 13, 7097–7114, doi: 10.5194/acp-13-7097-2013, 2013

Zhao, T. L., Gong, S. L., Zhang, X. Y., Blanchet, J. P., Mckendry, I. G., and Zhou Z. J.: A simulated climatology of Asian dust aerosol and its trans-pacific transport. Part I: mean climate and validation, J. Clim., 19(1), 104–122, doi: 10.1175/JCLI3606.1, 2006

Zhao, T. L., Gong, S. L., Huang, P., and Lavoue D.: Hemispheric transport and influence of meteorology on global aerosol climatology, Atmos. Chem. Phys., 12, 7609–7624, doi: 10.5194/acp-12-7609-2012, 2012.

Zhou, T. J., and Yu, R. C.: Twentieth century surface air temperature over China and the globe simulation by coupled climate models. J. Clim., 19(22), 5843–5858, 2006
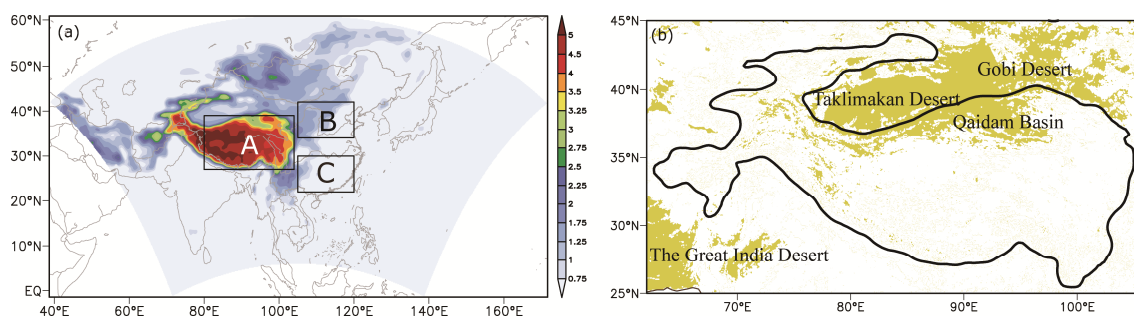
Figure 1: (a) Model domain and topography (units: km) and (b) dust source regions (yellow area) over the Tibetan Plateau and surrounding areas. Rectangles in (a) indicate areas Tibetan Plateau (A, 27–39°N, 80–105°E), north EASM region (B, 34–42°N, 105–120°E), and south EASM region (C, 22–30°E, 105–120°N).
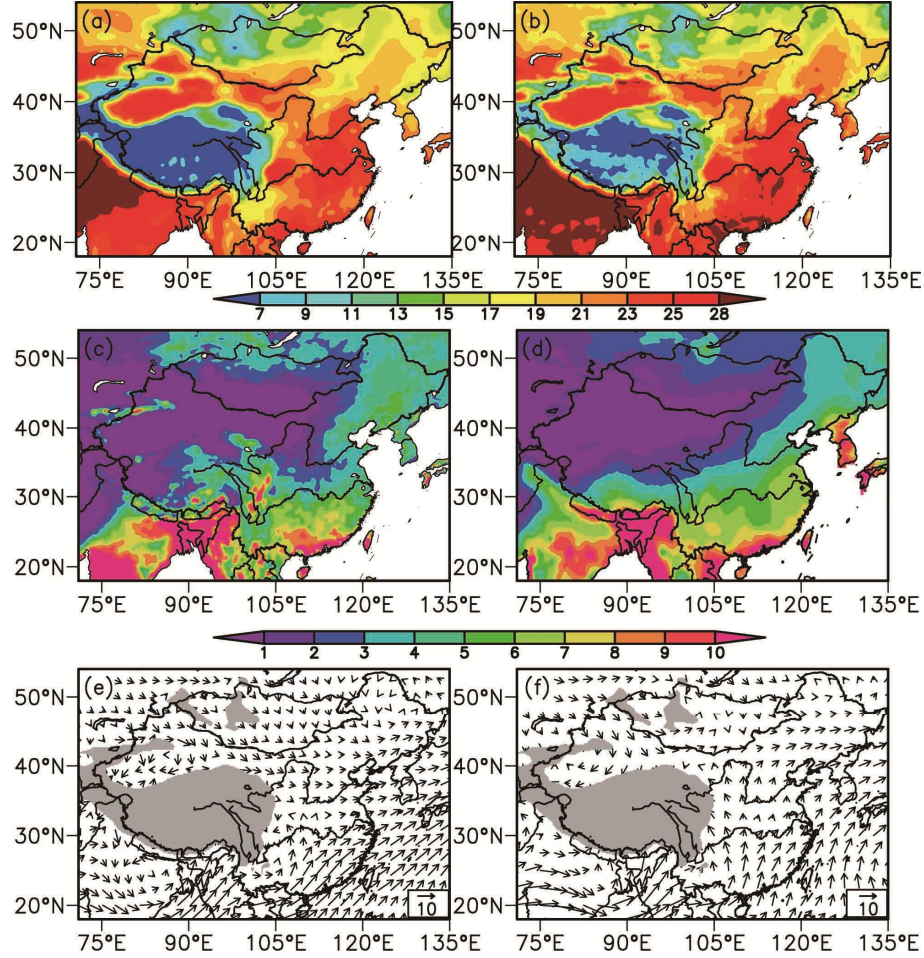
Figure 2: Spatial distribution of (a, b) **summer** surface air temperature (°C) and (c, d) **summer** precipitation (mm day^{-1}) simulated in the control experiment (left) and the CRU observations (right) for 1990–2009. The bottom two panels are wind vectors at 850 hPa simulated in (e) the control experiment and (f) the NCEP–DOE re-analysis during the summer monsoon season (June–August) averaged for 1990–2009.
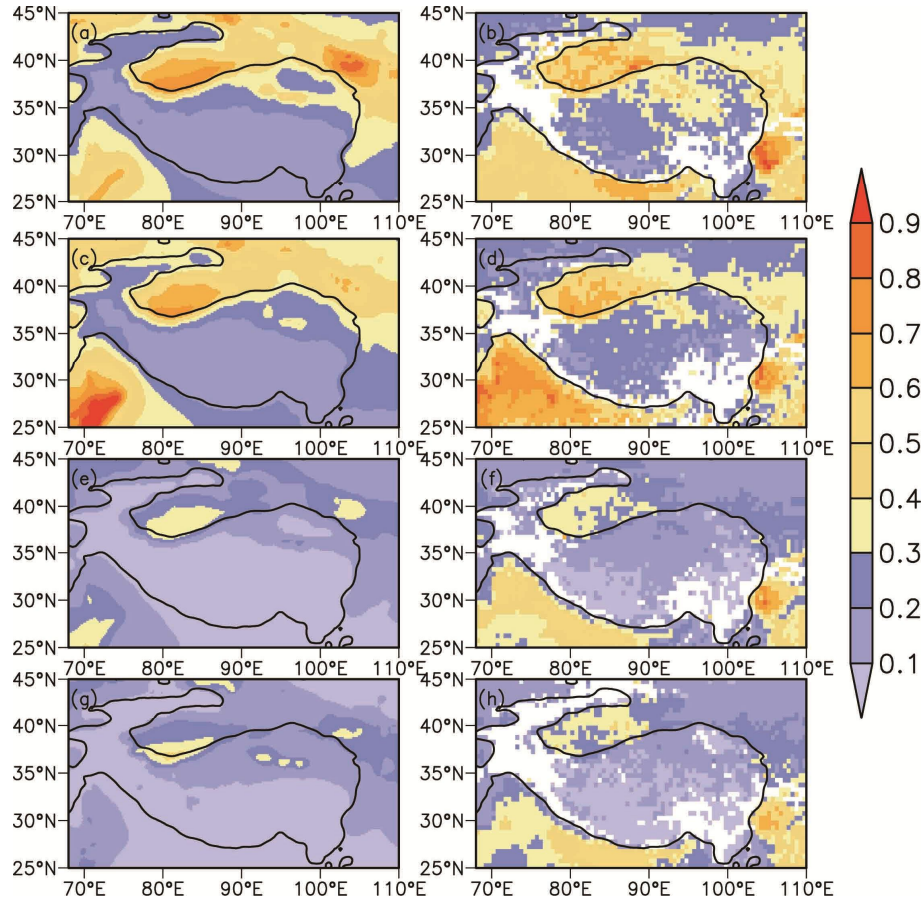
5   **Figure 3:** Spatial distribution of the dust AOD simulated by the control experiment (left panels) and the total aerosol optical depth observed by MISR at 550 nm (right panels) averaged in (a, b) spring, (c, d) summer, (e, f) autumn and (g, h) winter during the time period 2000–2009.
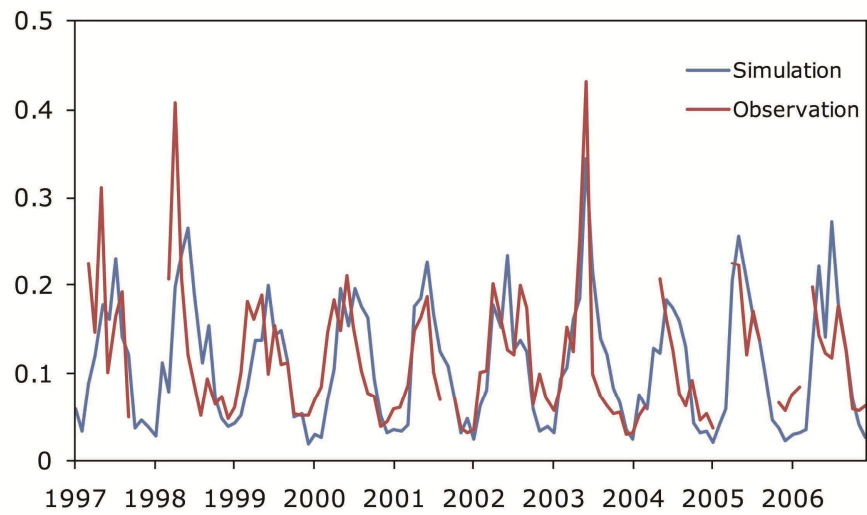
Figure 4: Comparison between the simulated variation of the monthly mean dust AOD in the control experiment and the AERONET-observed variation of the monthly mean aerosol AOD (500 nm) at Dalanzadgad from 1997 to 2006 (***R*=0.66**).
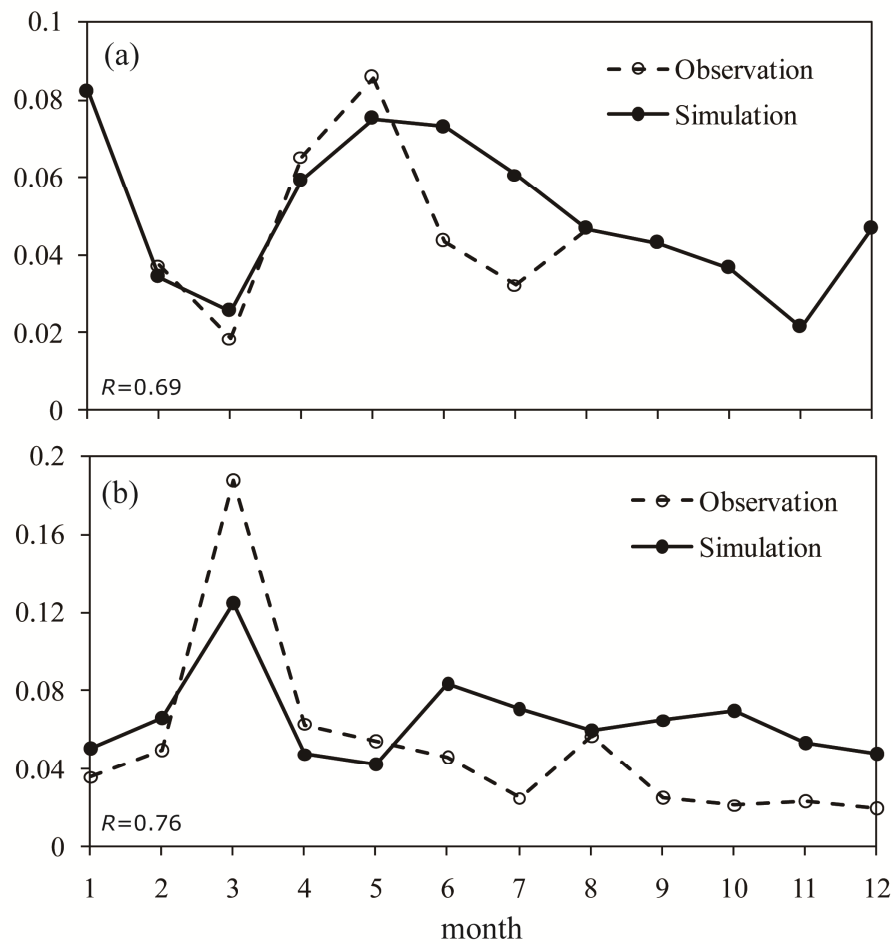
5 **Figure 5:** Comparison between the AERONET-observed monthly mean aerosol AOD (500 nm) at Nam Co and simulated by the control experiment at the grid near Nam Co in (a) 2007 and (b) 2009.
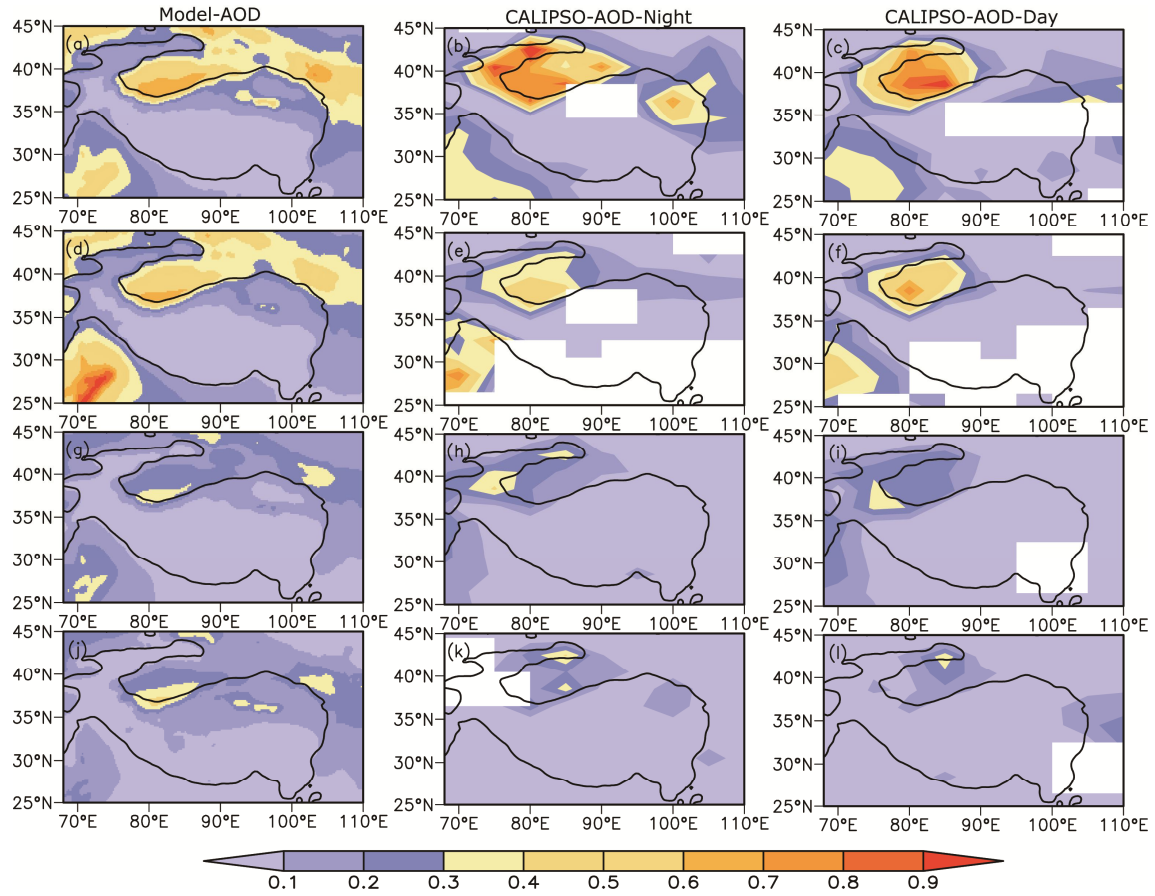
Figure 6: Spatial distribution of the dust AOD simulated by the control experiment (left panels) and observed by CALIPSO at night (middle) and during daytime (right panels) averaged in (a, b, c) spring, (d, e, f) summer, (g, h, i) autumn and (j, k, l) winter during the time period 2007–2009.
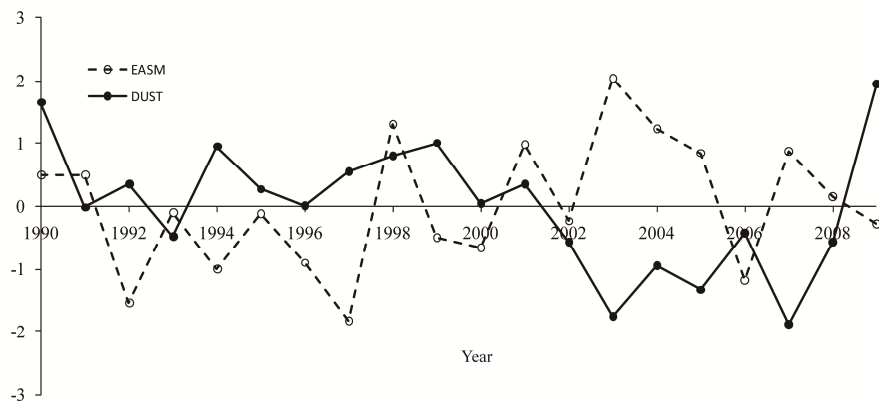
Figure 7: Difference (CON minus SEN) in the normalized regional mean dust column load averaged over the Tibetan Plateau (27–39°N, 80–105°E) and in the EASM index for summer during the period 1990–2009 ($R=-0.41$).
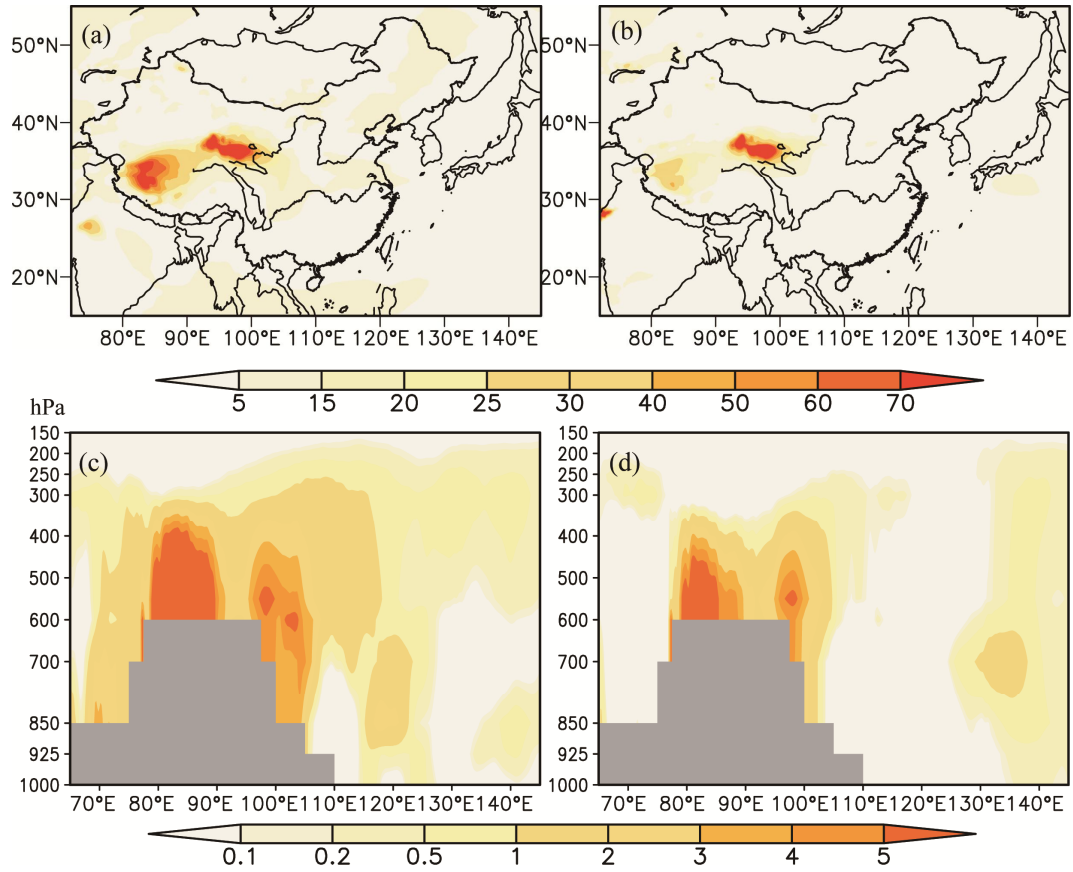
Figure 8: (a, b) Simulated differences (CON minus SEN) in the horizontal distribution of the column dust load (mg m^{-2}) and (c, d) the longitude–height cross-section (averaged over 32–36°N) of the dust mixing ratio (μg kg^{-1}) for summer in heavy (left) and light dust years (right).
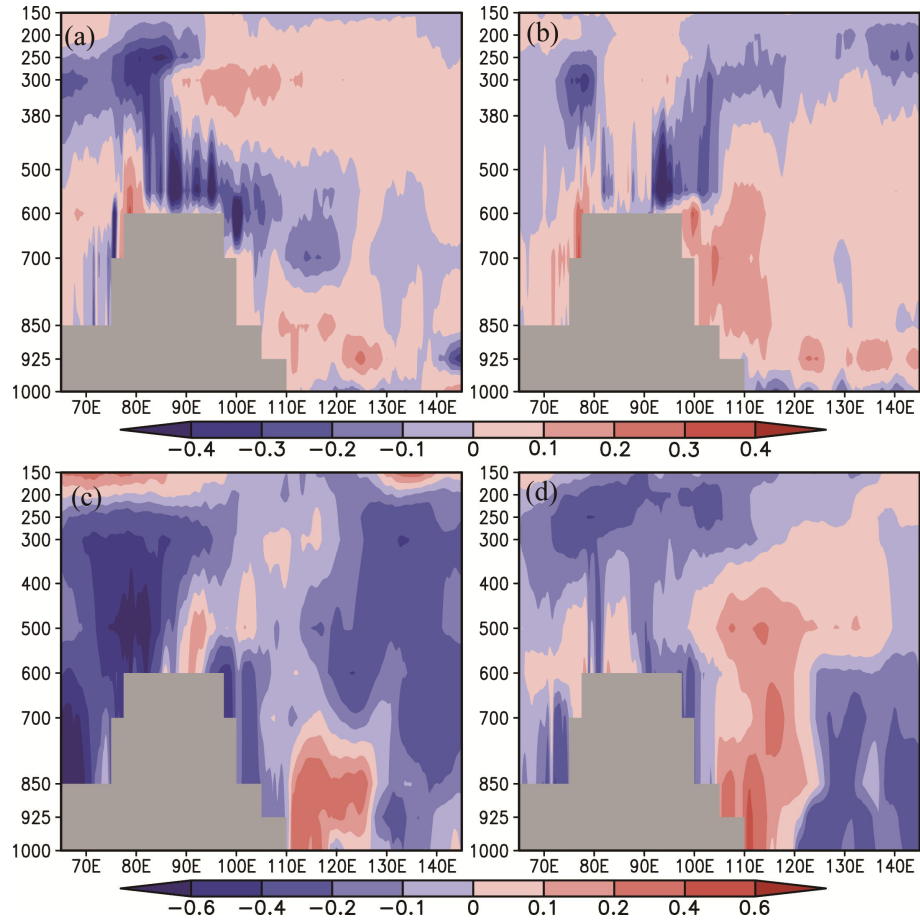
Figure 9: Longitudional cross-section of the differences between CON and SEN averaged over 32–36°N in summer. (a) and (b): net radiative cooling rate (short-wave heating rate + long-wave cooling rate, K day^{-1}) in heavy and light dust years respectively. (c) and (d): as (a) and (b) but for atmospheric temperature.
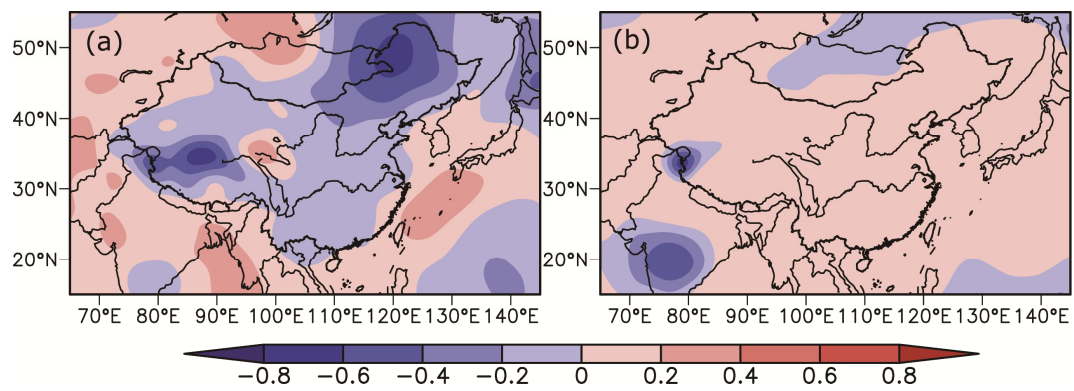
Figure 10: Simulated difference in summer surface temperature between CON and SEN in (a) heavy and (b) light dust years.
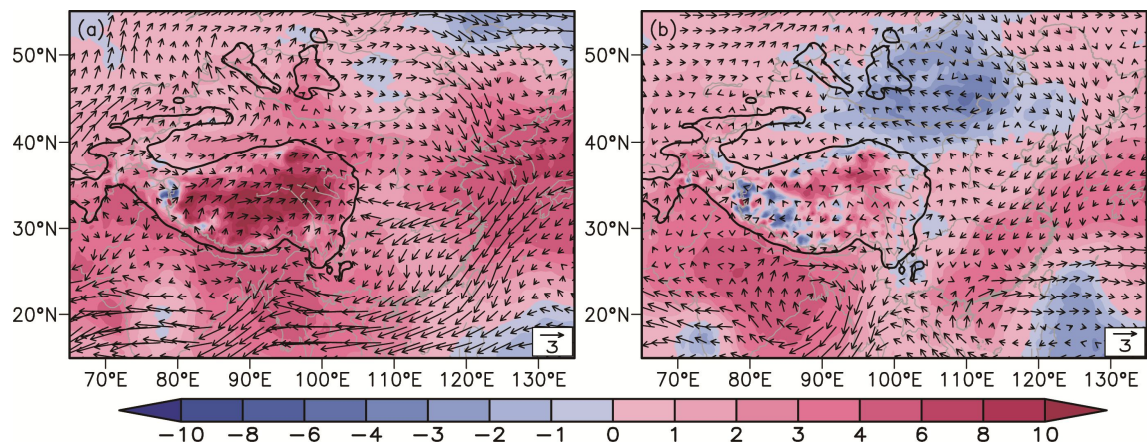
Figure 11: Simulated difference in atmospheric circulation at 850 hPa (vector, m s^{-1}) and geopotential height at 600 hPa (shaded, m) in summer between CON and SEN in (a) heavy and (b) light dust years.
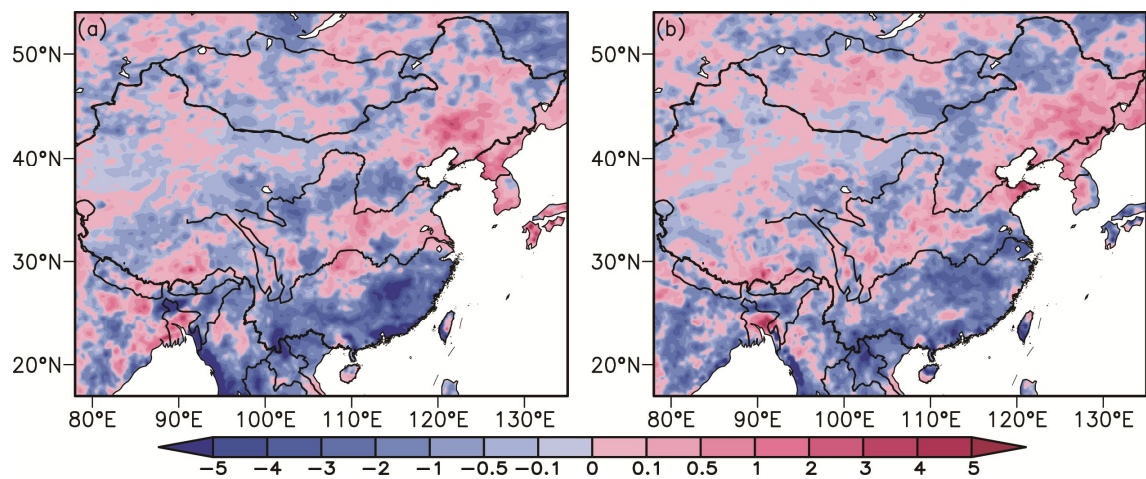
Figure 12: Simulated difference in summer precipitation between CON and SEN in (a) heavy and (b) light dust years.
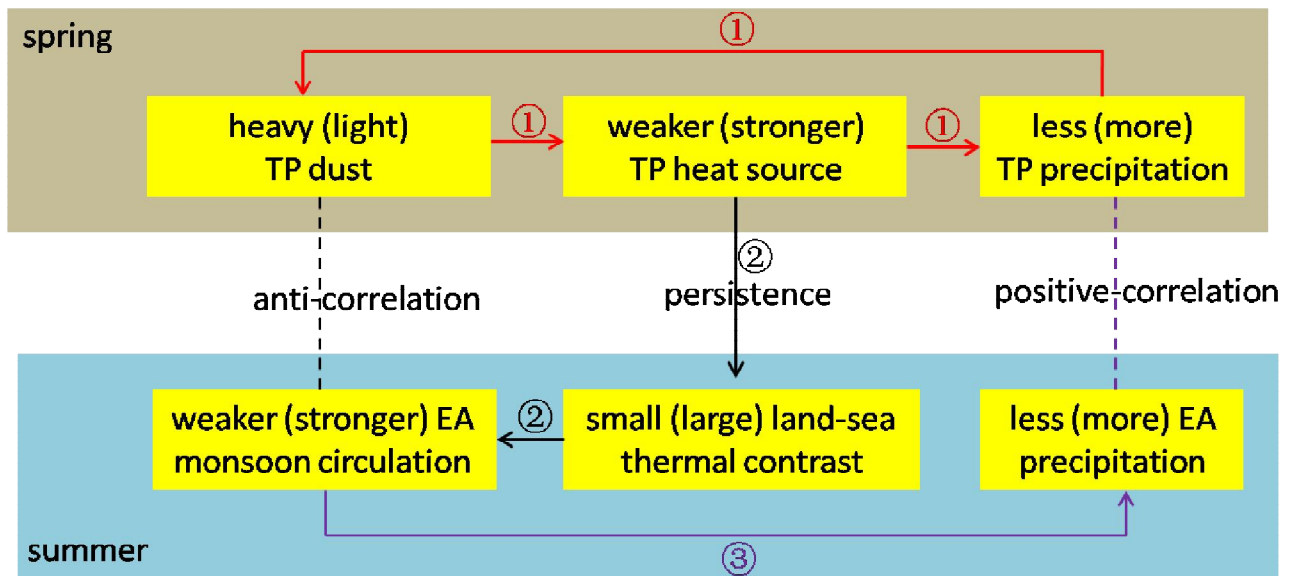
10 **Figure 13:** Schematic diagram showing the relation of dust aerosols emitted from the TP in spring with EASM precipitation.